International Conference on the Physics of Reactors "Nuclear Power: A Sustainable Resource"
Casino-Kursaal Conference Center, Interlaken, Switzerland, September 14-19, 2008

Recent Advances in the HELIOS-2 Lattice Physics Code

C.A. Wemple[a,*], H-N.M. Gheorghiu[b], R.J.J. Stamm'ler[c], E.A. Villarino[d]

[a] *Studsvik Scandpower, Inc., Idaho Falls, ID, USA*
[b] *Studsvik Scandpower, Inc., Boston, MA, USA*
[c] *Studsvik Scandpower AS, Kjeller, Norway (deceased)*
[d] *INVAP S.E., Bariloche, Argentina*

Abstract

Major advances have been made in the HELIOS code, resulting in the impending release of a new version, HELIOS-2. The new code includes a method of characteristics (MOC) transport solver to supplement the existing collision probabilities (CP) solver. A 177-group, ENDF/B-VII nuclear data library has been developed for inclusion with the new code package. Computational tests have been performed to verify the performance of the MOC solver against the CP solver, and validation testing against computational and measured benchmarks is underway. Results to-date of the verification and validation testing are presented, demonstrating the excellent performance of the new transport solver and nuclear data library.

1. Introduction

The two-dimensional collision probabilities transport code HELIOS (Casal, et al., 1991) has been a mainstay of the lattice physics analysis community since its initial release. With the release of the ENDF/B-VII cross section database (Chadwick, et al., 2006), it was decided that a major upgrade of the code was in order. The main features of the new code are:

- a characteristics transport solver;
- new ENDF/B-VII nuclear data library;
- improved temperature-dependent resonance treatment;
- improved geometric modelling capabilities.

This paper provides a description of the implementation and testing of these upgrades, which will be released as HELIOS-2.

2. Method of Characteristics (MOC) Solver

As an alternative to the collision probabilities method, a method of characteristics (MOC) solver has been added to the transport solver module. The MOC solution has been implemented both in the current coupled form (CCCM) and in the uncoupled (k=0) form (the so-called "long characteristics"). Because of reduced memory requirements, the "long characteristics" solution offers improved computational performance from the uncoupled collision probabilities solution and,

* Corresponding author, Charles.Wemple@studsvik.com
Tel: +1 208 522 1629; Fax +1 208 522 1187.

therefore, the potential for modeling larger, more complex geometries.

The method of characteristics as a solution to the neutron transport equation was first proposed nearly fifty years ago (Vladimirov, 1959; Marchuk, 1961). Since then, it has become widely used in neutral particle transport codes (Halsall, 1980; Knott, 1990, Postma and Vujic, 1999; Sanchez and Chetaine, 2000; Smith and Rhodes, 2002; Wu and Roy, 2003). A brief derivation of the characteristics equations as implemented in HELIOS-2 is provided here.

The derivation begins with the standard one-group characteristics equation along integration chord k with the constant cross section, flat-flux, and flat-source assumptions for region i:

$$\Phi_{i,k}(\tau,\vec{\Omega}) = \Phi_{i,k}^{in}(\vec{\Omega})e^{-\Sigma_{ti}\tau} + \frac{\Sigma_{si}\phi_i + Q_i}{4\pi V_i \Sigma_{ti}}(1-e^{-\Sigma_{ti}\tau}) \quad (1)$$

where τ denotes the distance along the direction Ω. The angular variable is discretized with each chord k having a directional angle θ with $\cos\theta = \mu$ and weight ω. The interface currents at each region boundary j may be integrated from the angular flux using the weights and directions of the characteristics:

$$J_{ij} = \sum_{k\cap j} \omega_k \mu_k \Phi_{i,k}^{out} \quad (2)$$

where J_{ij} is the current exiting region i through boundary j and the summation is over all chords k intersecting boundary j. The region-averaged flux may then be found from the following balance equation:

$$\Sigma_i V_i \phi_i = \Sigma_{si}\phi_i + Q_i + J_i^{in} - J_i^{out}, \quad (3)$$

with the total in and out currents defined as:

$$J_i^{in} - J_i^{out} = \sum_j J_{ij} - \sum_j J_{ji} \ . \quad (4)$$

In Eq. (4), J_{ij} is the current entering region i through boundary j. An initial guess for the in-currents is obtained by assuming an isotropic flux at the boundary surfaces.

To accelerate the convergence of the characteristics solution, a pseudo-diffusion solution may be performed (Lee, et al., 2000). If the currents are expressed as:

$$J_{ij} = a_{ij}\phi_j \ , \quad (5)$$

then Eq. (3) may be re-written in the following form:

$$\left(\Sigma_{ri}V_i + \sum_j a_{ij}\right)\phi_i = Q_i + \sum_j a_{ji}\phi_j \ , \quad (6)$$

where Σ_{ri} is the removal cross section (total – self-scatter) for region i. This bears a strong resemblance to the diffusion equation and can be easily solved for the region fluxes, once the coefficients a_{ij} are known. The coefficients are dependent on the transport solution and a reasonable solution to Eq. (6) requires that these coefficients be relatively stable; thus, an additional convergence test is performed between characteristic sweeps to determine the variation of the coefficients. The diffusion-like solution is only applied when the variation in the coefficients between transport sweeps is less than the flux convergence criterion.

The solution scheme for the method of characteristics as implemented in HELIOS-2 is shown in Figure 1. The procedure shown in this figure occurs inside the standard eigenvalue (outer) iteration scheme. Convergence tests are performed on both the currents and the fluxes to assure that both quantities are adequately converged.

This iteration procedure is performed for each element defined in the geometry. Current coupling between elements is exactly as described for the collision probabilities solution, with the exception that only azimuthal (i.e., single polar angle) current coupling is allowed presently.

In the collision probabilities method, the integration over the polar angle is performed explicitly during the computation of the response fluxes. In the method of characteristics, the discretization of the angular variable must be performed in the full angular domain, i.e., both azimuthal and polar angles; this requires careful selection of the angular quadrature used to perform the polar angle integration.

Because of the large number of azimuthal angles typically used to assure accuracy in the 2D geometric (area and volume) integrations, it is desirable to minimize the number of discrete polar

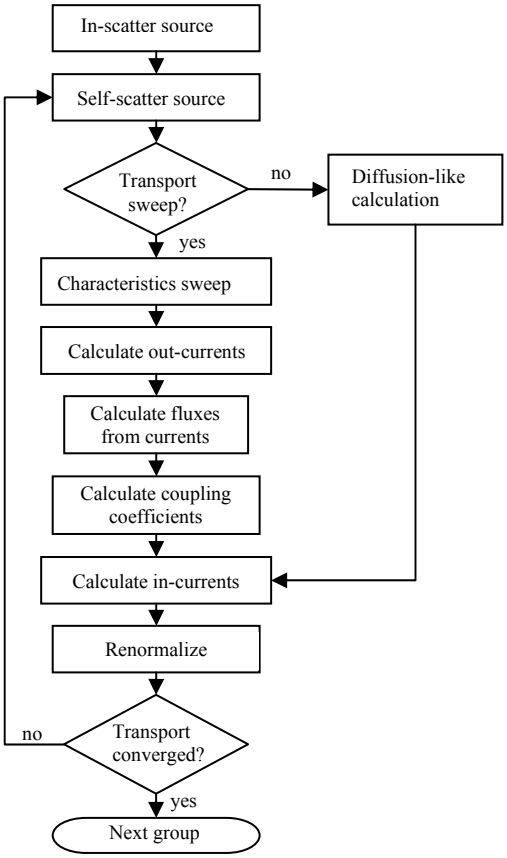

Figure 1. The calculation scheme for the MOC transport solver in HELIOS-2.

angles used. Improved methods for performing this minimization effort are constantly being introduced and are well documented in the literature (Leonard and McDaniel, 1995; Sanchez, et al., 2002; Tabuchi, et al., 2005). To permit maximum flexibility in the characteristics implementation, several quadrature sets were selected and included in HELIOS-2.

3. ENDF/B-VII Cross Section Library

The HELIOS-2 neutron data library is based on ENDF/B-VII R0 evaluated data files (Chadwick, et al., 2006), the most comprehensive evaluations available. The main cross section processing was performed using the NJOY code (MacFarlane and Muir, 1994), version 99.161. Several modifications were made to this code, including the addition of a module that uses NJOY-generated data to build the resonance integral data required for the HELIOS library format. The auxiliary code, HEBE, was used to assemble the processed isotope cross sections and resonance integral data into the final library. The new library contains neutron data for 303 materials, including 121 fission products and 40 actinides, with 80 resonance materials. The upper limit of the resonance region was increased from 9.119keV to 111.1keV. Photon cross section data are available for 301 materials. The base nuclear data library uses 177 neutron groups and 48 photon groups; a production library with 49 neutron groups and 18 photon groups is also being developed.

Many natural elements (Si, Cd, etc.) once present in ENDF/B-VI are no longer in the ENDF/B-VII evaluations, but it was desired to retain the elemental definitions in the library. In these cases, the isotopic constituents of the natural elements were processed with NJOY and HEBE was used to mix them according to their natural abundances to generate the elemental data for the library. Several elements (Zr, Cr, Fe, Ni) presented a special challenge, because they are now treated as resonance materials with resonance data for each isotope; the individual isotopes were processed as resonance isotopes and fictitious identifiers were created for the natural elements, to signal the input processor to parse it into the isotopes with their natural abundances.

4. Other Improvements

Several other, less massive, upgrades were also implemented. An improved method for treating resonance cross sections in regions with a non-uniform temperature profile (e.g., fuel pins) was implemented (Wemple, et al., 2007). Capabilities allowing the user to edit scattering matrix moments up to P3 were added. Additional improvements targeted the geometric modeling capabilities and material composition inputs for burnable absorbers.

5. Verification Testing Results

Verification testing of the MOC solver has been very successful. Runtimes in the current coupled mode are generally a factor of 2-5 longer than the comparable CCCP calculations; this was expected and not the principal focus of the upgrade. Runtimes for explicitly-coupled (k=0) calculations

are up to a factor of 10 shorter than corresponding CP calculations and memory requirements are reduced by as much as an order of magnitude.

Computational results for the verification tests are excellent, with differences of only a few pcm in most cases. Results of the verification test matrix are shown in Figures 3 and 4, displaying the comparison of the MOC solution with the CP solution. This test matrix is a collection of fuel bundle and pin-cell calculations for a wide variety of reactor configurations. The differences for the MTR and Dry MOX cases are a result of accumulation of differences with burnup; both calculations are carried out to very high burnup levels.

Table 1 shows a timing and memory comparison for the test matrix BWR fuel assembly depletion case, using both current coupled and explicitly coupled MOC and CP calculations, and for a PWR multi-assembly depletion calculation with current coupling. The reductions in computation time and memory usage for the explicitly coupled case demonstrate the advantages of the long-characteristics calculation; this was the main driver for the MOC implementation.

6. Selected Validation Testing Results

Validation testing involves both the new code and the nuclear data library, and is focussed on comparisons to measurements, supplemented by computational benchmarks. Both integral results and isotopic measurements are included in the array of validation tests; the full validation suite is still being populated as of the writing of this paper. Selected results are presented here.

6.1. Yankee Rowe Isotopics

The Yankee Rowe isotopics measurements (Nodvik, 1966; Nodvik, 1969) were conducted by the Atomic Power Division of Westinghouse in the 1960's and have been used in prior code benchmarking efforts. The measurements were destructive assays of a total of 71 fuel rods from the Yankee Rowe PWR plant Cores I-IV to determine burnup and actinide isotopics. These rods were selected from 16 fuel assemblies scattered throughout the core. Multiple rods were extracted from each assembly, with locations selected to provide a mixture of spectra. Multiple axial locations were sampled for each rod, selected to avoid the perturbed locations near the grid plates and the top and bottom of the rods. Figure 2 shows the assembly and rod locations selected.

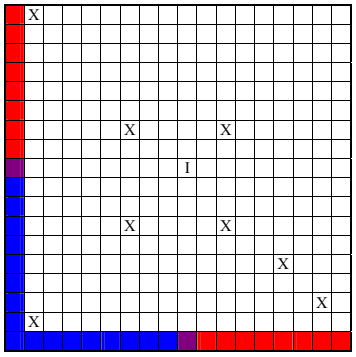

Figure 2. Locations of pins sampled in Yankee Rowe assembly (X), with control blade locations shown for Type A (blue) and Type B (red) assemblies.

The fuel rods are UO2 clad with stainless steel; the pin outer diameter is 0.34 inches with a clad thickness of 0.021 inches and pellet diameter of 0.294 inches. Pin pitch is nominally 0.422 inches; however, the outer row of pins adjacent to the control blades has a pitch of 0.456 inches. The assembly pitch is 7.66 inches.

Depletion calculations were performed to 45000 MWd/kg using core-averaged power densities. The HELIOS-2 model included both assembly types with periodic boundary conditions, to simulate an infinite reactor core. The large number of individual samples, the wide burnup range involved, and the lack of detailed assembly exposure history data, made independent calculation of each assembly sampled impractical. Isotopic concentration edits for actinide isotopes (^{234}U to ^{244}Cm) were obtained for the pin locations indicated in Figure 2.

In all graphs, the data points are the measured values and the curves denote the calculated results. The results in all plots are ordered by decreasing correspondence to the asymptotic assembly spectrum. Two sets of data are shown for the measurements – those labeled "WCAP small" are small-pitch (0.422 in.) locations at the interior of the assembly and those labeled "WCAP large" are large-pitch (0.456 in.) locations near the exterior of the assembly. In general, the interior pins (locations (12,7) and (7,7)) correspond to the small pitch measurements; the exterior pins (locations

(17,2) and (1,2)) correspond to the large pitch measurements; and the remaining pins (locations (14,15) and (16,17)) fall between the extremes. Isotopic concentration comparisons with measured data for several relevant nuclides (^{235}U, ^{239}Pu, ^{241}Pu, ^{242}Pu) are shown in Figures 5-8; agreement with the measurements is excellent.

6.2. "Strawbridge and Barry" Criticals

The so-called Strawbridge and Barry criticals (Strawbridge and Barry, 1965) have served as test cases for reactor physics for decades. This collection of 116 critical and exponential experiments, comprising 55 UO2 and 61 U metal lattices, is a compilation of experiments performed at various facilities during the late 1950's and early 1960's. They include variations in cell geometry, clad material, moderator composition, and fuel enrichment; it is this variety that makes them a suitable testing ground for codes and data libraries. For these tests, 101 of the 116 criticals were analyzed; the 15 cases with mixed light and heavy water moderator were excluded.

A summary of the results for the 101 criticals in this series is shown in Table 2. The new library raises the average k_{eff} by over 600pcm and generally produces results closer to critical. Only the dissolved boron cases have an average k_{eff} below 1.0 and only the unclad U metal cases have an average deviation from critical greater than 400pcm. The standard deviations for both libraries generally agree within a few percent; considering the great variety of configurations examined, the data scatter is more a function of the critical configurations than the nuclear data library.

7. Summary and Conclusions

A major upgrade of the HELIOS code, to be released as HELIOS-2, has been undertaken. The main components of the upgrade are the implementation of the MOC transport solver and the creation of a new ENDF/B-VII cross section library. Verification and validation testing to-date demonstrates excellent performance for the new MOC solver and nuclear data library. Extensive validation testing is still ongoing. Release of the new code suite is planned for the fall of 2008.

References

Askew J R (1972) "A Characteristics Formulation of the Neutron Transport Equation in Complicated Geometries," AAEW-M 1108, United Kingdom Atomic Energy Establishment.

Casal J J, Stamm'ler R J J, Villarino E A, and Ferri A A (1992) "HELIOS: Geometric Capabilities of a New Fuel-Assembly Program," *Proc. Int. Top. Mtg. Adv. Math. Comp. Reac. Phys.,* Pittsburg, PA, USA, Vol. II, Sect. 10.2.1, 1-13.

Chadwick M B, et al. (2006) "ENDF/B-VII.0: Next Generation Evaluated Nuclear Data Library for Nuclear Science and Technology," *Nuclear Data Sheets* **107**, 2931.

Halsall M J (1980) "CACTUS, A Characteristics Solution to the Neutron Transport Equations in Complicated Geometries," AAEW-R 1291, United Kingdom Atomic Energy Establishment.

Knott D (1990) "KRAM: A Lattice Physics Code for Modeling the BWR Fuel Designs", Ph.D. Thesis, The Pennsylvania State University.

Lee G S, Cho N Z, and Hong S G (2000) "Acceleration and Parallelization of the Method of Characteristics for Lattice and Whole-Core Heterogeneous Calculation," *Proc. Intl. Conf. Physics of Reactors (PHYSOR 2000),* Pittsburg, PA, USA.

Leonard A and McDaniel C T (1995) "Optimum Polar Angles and Weights," *Trans. Am. Nucl. Soc.* **73**, 171.

Macfarlane R E and Muir D W (1994) "The NJOY Nuclear Data Processing System, Version 91," LA-12740-M, Los Alamos National Laboratory.

Marchuk G I (1961) "A Survey of Nuclear-reactor Design Methods," *Atomnaya Energiya* **11** (4), 356.

Nodvik R J (1966) "Evaluation of Mass Spectrometric and Radiochemical Analyses of Yankee Rowe Core I Spent Fuel," WCAP-6068, Westinghouse Electric Corp., Atomic Power Division.

Nodvik R J (1969) "Supplementary Report on Evaluation of Mass Spectrometric and Radiochemical Analyses of Yankee Rowe Core I Spent Fuel, Including Isotopes of Elements Thorium Through Curium,"

WCAP-6086, Westinghouse Electric Corp., Atomic Power Division.

Postma T and Vujic J (1999) "The Method of Characteristics in General Geometry with Anisotropic Scattering," *Proc. Intl. Mtg. Mathematics and Computation, Reactor Physics and Environmental Analysis in Nuclear Applications (M&C 1999)*, Madrid, Spain.

Sanchez R and Chetaine A (2000) "A Synthetic Acceleration for a Two-Dimensional Characteristic Method in Unstructured Meshes," *Nucl. Sci. Eng.* **136**, 122-139.

Sanchez R, Mao L, and Santandrea S (2002) "Treatment of Boundary Conditions in Trajectory-Based Deterministic Transport Methods," *Nucl. Sci. Eng.* **140**, 23-50.

Smith K S and Rhodes III J D (2002) "Full-Core, LWR Core Calculations with CASMO-4E," *Proc. Intl. Conf. Physics of Reactors (PHYSOR 2002)*, Seoul, Korea.

Strawbridge L E and Barry R F (1965) "Criticality Calculations for Uniform Water-Moderated Lattices," *Nucl. Sci. Eng.* **23**, 58-73.

Tabuchi M, Yamamoto A, Endo T, Sugimura N, Ushio T, and Mori M (2005) "Yet Another Optimum Polar Angular Quadrature Set for the Method of Characteristics," *Trans. Am. Nucl. Soc.* **93**, 506.

Vladimirov V S (1959) Ph.D. Dissertation, V.A. Stecklova Mathematics Institute, USSR. Quoted by Marchuk (1961).

Wemple C A, Stamm'ler R J J, and Ferri A A (2007) "Improved Temperature-Dependent Resonance Treatment in HELIOS-1.9," *Trans. Am. Nucl. Soc.* **96**, 657.

Wu G J and Roy R (2003) "A New Characteristics Algorithm for 3D Transport Calculations," *Annals of Nucl. Energy* **30**, 1-16.

Table 1. Timing and memory comparison for single-assembly BWR and multi-assembly PWR calculations.

Solution Method	Parameter	BWR (70 State Points)		PWR (56 SPs)
		Current coupling (k=4)	Explicit coupling (k=0)	Current coupling (k=4)
CP	CPU time (min.)	2.19	2813	421
	Wall clock time (min.)	2.2	2876	742
	Memory (Mwords)	102	225	2009
MOC	CPU time (min.)	14.37	162	774
	Wall clock time (min.)	14.4	165	779
	Memory (Mwords)	15	80	284

Table 2. Comparison of k-effective for Strawbridge and Barry criticals with ENDF/B-VI and ENDF/B-VII libraries.

Description of Cases	Number of Cases	ENDF/B-VI Library		ENDF/B-VII Library		E7-E6 (pcm)
		Avg. k-eff	Std. Dev.	Avg. k-eff	Std. Dev.	
Hexagonal	74	0.99623	0.00674	1.00306	0.00653	683
Square	27	0.99614	0.00761	1.00130	0.00788	516
Aluminum clad	56	0.99493	0.00511	1.00188	0.00510	695
Stainless steel clad	25	0.99549	0.00743	1.00053	0.00749	504
No clad (U metal)	20	1.00068	0.00907	1.00715	0.00878	647
Dissolved boron	7	0.99446	0.00269	0.99882	0.00308	436
No boron	94	0.99634	0.00715	1.00287	0.00705	653
UO_2 fuel	40	0.99531	0.00721	1.00094	0.00733	563
U metal fuel	61	0.99680	0.00677	1.00367	0.00647	687
All cases	101	0.99621	0.00695	1.00259	0.00692	638

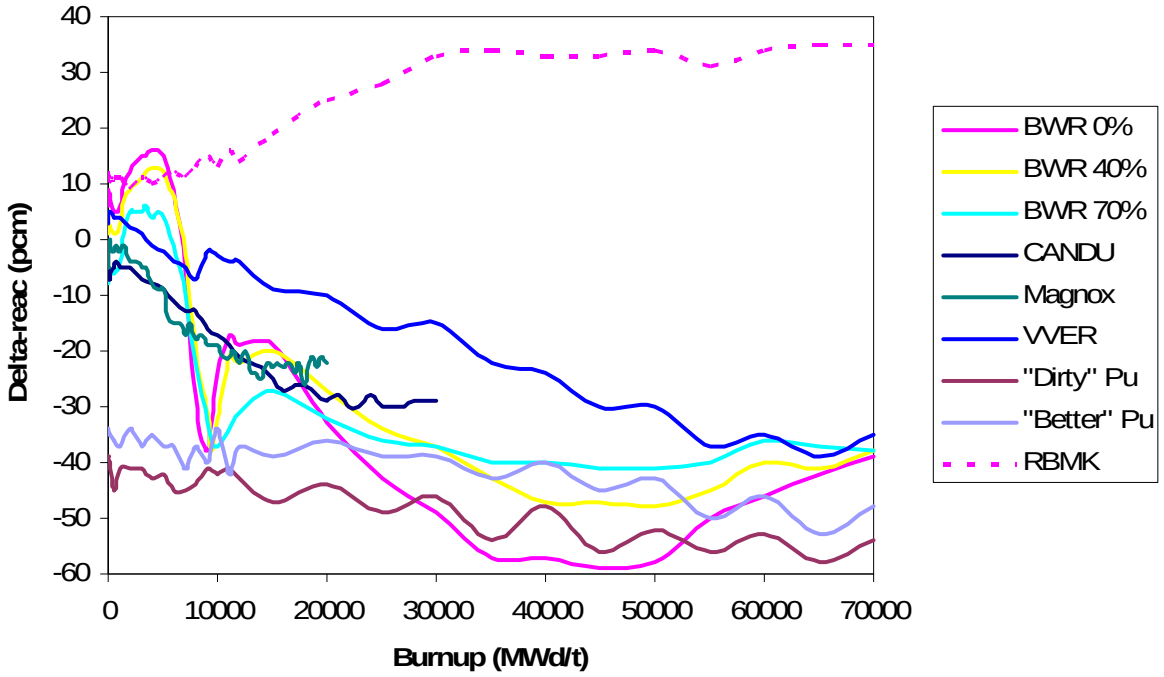

Figure 3. Results of test matrix calculations, comparing MOC to CP.

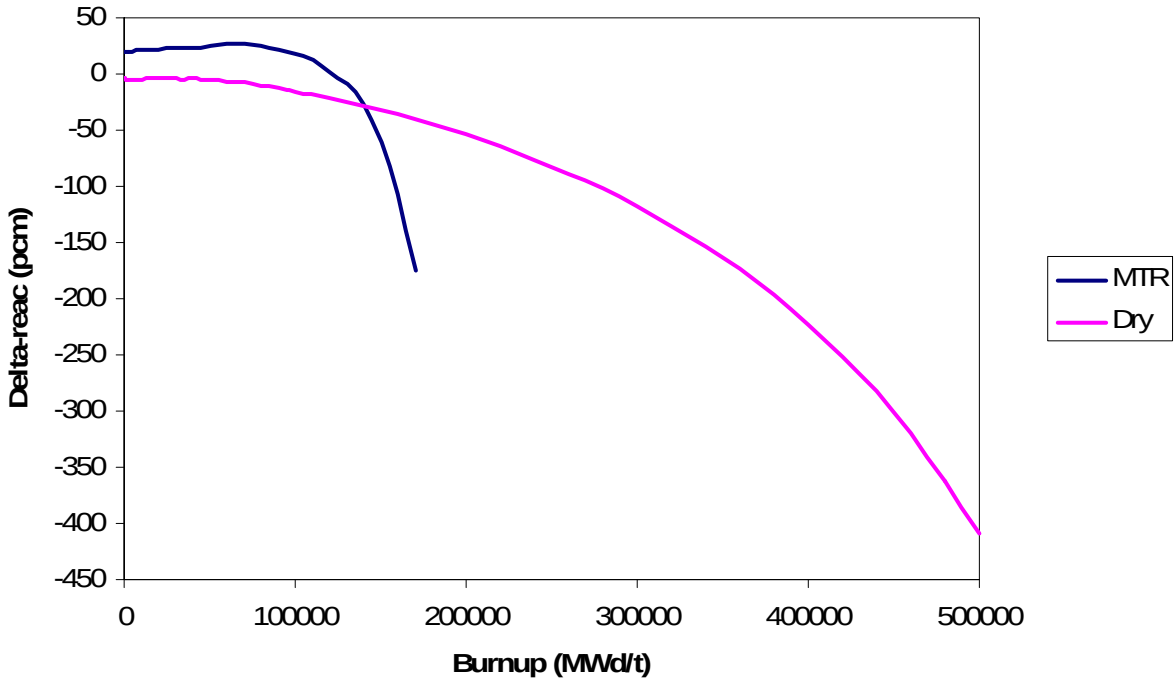

Figure 4. Results of test matrix MTR assembly and Dry MOX pin-cell calculations, comparing MOC to CP.

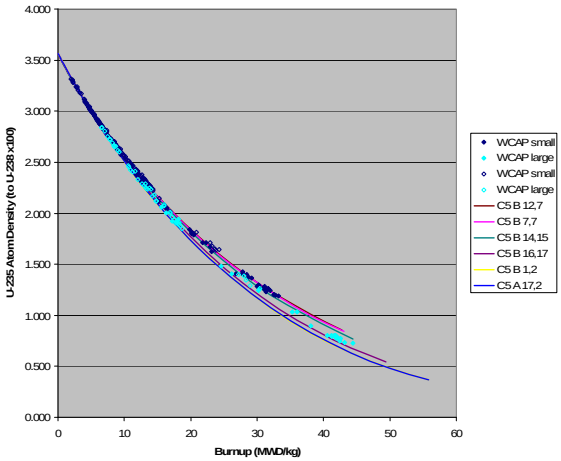

Figure 5. Yankee Rowe ^{235}U concentration relative to initial ^{238}U concentration.

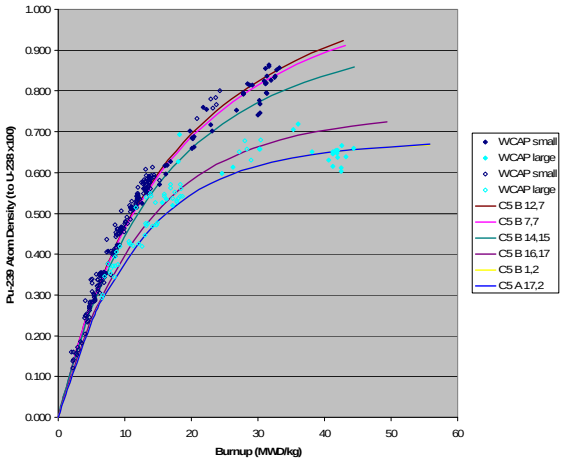

Figure 6. Yankee Rowe ^{239}Pu concentration relative to initial ^{238}U concentration.

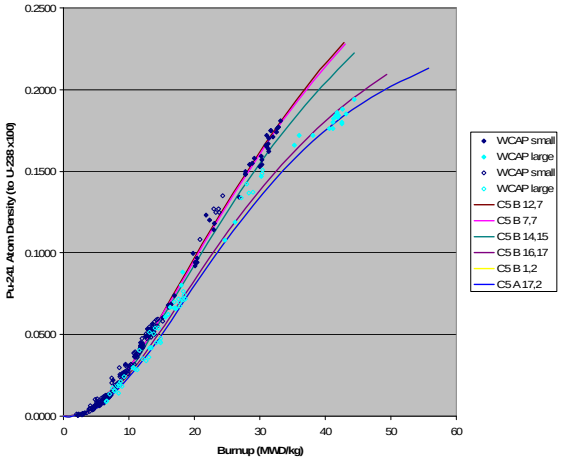

Figure 7. Yankee Rowe ^{241}Pu concentration relative to initial ^{238}U concentration.

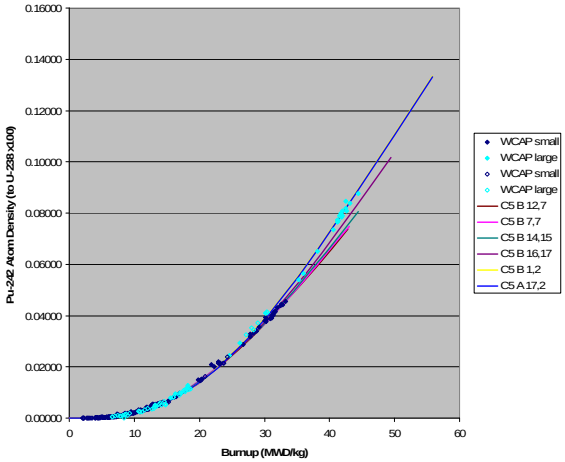

Figure 8. Yankee Rowe ^{242}Pu concentration relative to initial ^{238}U concentration.